17th World Conference on Earthquake Engineering, 17WCEE
Sendai, Japan - September 13th to 18th 2020

A BENCHMARK TEST FOR MICROTREMOR EXPLORATIONS: PHASE VELOCITY FOR IRREGULAR SUBSURFACE STRUCTURES

M. Ohori[(1)], H. Uebayashi[(2)], I. Cho[(3)], H. Arai[(4)], K. Yoshida[(5)], H. Suzuki[(6)], H. Takahashi[(7)], Y. Hagiwara[(8)], A. Nobata[(9)], T. Hayakawa[(10)], T. Hayashida[(11)], T. Yokoi[(12)], S. Kishi[(13)], T. Sekiguchi[(14)], K. Kojima[(15)], S. Ling[(16)], K. Motoki[(17)], H. Nakagawa[(18)], T. Noguchi[(19)], K. Tsuchida[(20)], and M. Nagano[(21)]

[(1)] *Associate Professor, Univ. of Fukui, Japan, ohorim@u-fukui.ac.jp*
[(2)] *Associate Professor, Kyoto Univ., Japan, uebayashi.hirotoshi.8x@kyoto-u.ac.jp*
[(3)] *Senior Researcher, Geological Survey of Japan, AIST, Japan, ikuo-chou@aist.go.jp*
[(4)] *Chief Research Engineer, Building Research Institute, Japan, arai@kenken.go.jp*
[(5)] *Senior Researcher, Geo-Research Institute, Japan, yoshida@geor.or.jp*
[(6)] *Senior Researcher, Oyo Co., Japan, suzuki-haruhiko@oyonet.oyo.co.jp*
[(7)] *Associate Professor, Meijo Univ., Japan, hirohito@meijo-u.ac.jp*
[(8)] *Chief Research Engineer, Obayashi Co., Japan, hagiwara.yoshinori@obayashi.co.jp*
[(9)] *Senior Engineer, Obayashi Co., Japan, nobata.arihide@obayashi.co.jp*
[(10)] *Senior Researcher, Shimizu Co., Japan, takashi.hayakawa@shimz.co.jp*
[(11)] *Senior Research Scientist, Building Research Institute, Japan, takumi-h@kenken.go.jp*
[(12)] *Director of IISEE, Building Research Institute, Japan, tyokoi@kenken.go.jp*
[(13)] *Engineer, Fujita Co., Japan, shunsuke.kishi@fujita.co.jp*
[(14)] *Associate Professor, Chiba Univ., Japan, tsekiguc@faculty.chiba-u.jp*
[(15)] *Professor, Univ. of Fukui, Japan, k_kojima@u-fukui.ac.jp*
[(16)] *President, Geo-Analysis Institute Co., Japan, sqling818@yahoo.co.jp*
[(17)] *Senior Manager, Kobori Research Complex Inc., Japan, kmoto@kobori-takken.co.jp*
[(18)] *Senior Research Engineer, Building Research Institute, Japan, hiroto-n@kenken.go.jp*
[(19)] *Assistant Professor, Tottori Univ., Japan, noguchit@cv.tottori-u.ac.jp*
[(20)] *Scientist, Hanshin Consultants Co., Japan, tsuchida@hanshin-consul.co.jp*
[(21)] *Professor, Tokyo Univ. of Science, Japan, nagano-m@rs.noda.tus.ac.jp*

Abstract

This study quantitatively evaluates the applicability of the microtremor exploration method on irregular subsurface structures by performing a benchmark test using simulated microtremor waveform data calculated by the three-dimensional finite-difference method. The structure models used included a sediment-layered bedrock with an inclined subsurface connecting 450-m deep shallow bedrock with 1350-m deep bedrock. Simulated microtremors were induced by oblique forces on the surface equally aligned along the surrounding four model edges. For three models with different inclined angles of 5°, 10°, and 90°, arrays expanding from 200 m to 1600 m in the shortest sensor distance were deployed at thin-layered, thick-layered, and transition regions, respectively. The S-wave velocity was 1 km/s for the sediment and 3 km/s for the bedrock, so this high-velocity contrast induced the excitation of the first higher mode of the Rayleigh wave rather than the fundamental mode in a particular frequency range. Participants were requested to submit Rayleigh-wave phase velocity results for nine cases from vertical components. Rayleigh-wave phase velocity results from all participants showed a small deviation and reproduced the theoretical dispersion curves well from the surface-wave field and those from the full-wave field, except the case where the array was located on a transition region with an inclined angle of 90°. This benchmark test showed the potential applicability of the microtremor exploration method up to the inclined angle of 10°, which was larger than a criterion of an inclined angle of 5°, as suggested in previous studies.

Keywords: Benchmark Test, Microtremor Explorations, Phase Velocity, FK Method, SPAC Method

1. Introduction

Since the pioneering works by Aki [1] and others [2-4], the estimation of phase velocity from microtremor array observations and its usage for underground structure estimation have been accepted by many researchers, and its applications have accumulated [e.g., 5-9]. However, because the source of microtremors is not clear, it is important to clarify the applicable range when using microtremors as an underground structure exploration method. In contrast, as the applications of microtremor array measurements increase, the number of studies on sedimentary grounds with irregularities in the basement has also increased [10-13]. To understand better the characteristics of microtremors obtained by field observation, it is becoming more important to use numerical simulations of microtremors to perform array analysis under conditions where the source and underground structure are known and to examine the reliability of the information on the extracted underground structure [14-16].

The purpose of this research project is to examine and verify the effects of differences in data processing processes on microtremor array analyses using simulated microtremor waveforms calculated for an irregular ground structure model. We conducted two stages of numerical experiments. The first stage is called a benchmark test. Microtremor simulation waveforms were synthesized for a simple irregular ground model in which two layered bedrocks with different basement depths were connected by an inclined subsurface. The participants were requested to estimate the phase velocities, and the details of the underground structure model and site locations were presented to the participants in advance [17-20]. The second stage is called a blind test where microtremor simulation waveforms were synthesized using a more realistic three-dimensional velocity structure model: the Osaka sedimentary basin model. The participants were requested to estimate the phase velocities and the S-wave velocity structure models, but the details were not available except that the Osaka sedimentary basin model was used [21, 22]. In this article, we report the results of the benchmark test.

As a previous study similar to the benchmark test introduced in our project, a blind prediction on microtremor was performed as an event of the 3rd ESG International Symposium in 2006. The Effects of Surface Geology on Seismic Motion (ESG) has been a part of the International Association of Seismology and Physics of the Earth's Interior and the International Association of Earthquake Engineering since 1987. This is a joint research project and is still ongoing as a research project in an international framework. The overview of the ESG blind prediction is described in detail by Cornou et al. [23] and summarized by Kudo [24]. Although the ESG's blind prediction was a preceding study of this research project, the simulation waveform of the microtremor distributed to the participants was calculated using the analytical code of the Green's function developed by Hisada [25], and the underground structure model was a stratification structure. In addition, microtremor observation waveforms obtained by field observation were also distributed. This project focuses on the applicability of the microtremor exploration method considering an irregular subsurface structure and simulation waveforms of microtremors distributed to participants to be created using the three-dimensional finite-difference method [26]. After the ESG's blind prediction, new blind tests and reviews by researchers in Europe, the United States, and Australia induced vigorous efforts to create guidelines for the use of microtremors [27-31].

2. Overview of the benchmark test

2.1 Target model and provided simulated tremor waveform

Fig. 1 shows the model of the irregular ground structure that is the subject of the benchmark test. This model is a simple three-dimensional underground structure model in which two sedimentary layers with different thicknesses of sedimentary layers are connected by an inclined base surface, and the model uses the inclination angle θ of the inclined base surface as a parameter. A simulated tremor (velocity) waveform generated by exciting multiple points on the ground surface along the outer circumference of this model was

calculated using the three-dimensional finite-difference method [26]. The model volume in the difference method was 84 km in two horizontal directions and 25.5 km in the depth direction. The excitation points (episodes) were arranged at equal intervals (5 km) around the model (7 km inside the edge) for a total of 56 points). There were three calculation cases: θ = 5°, 10°, and 90°. A single excitation force was applied to each excitation point, and the component ratio in the x-, y-, and z-directions was set to 1:1:2, respectively. The frequency characteristic (amplitude) of the excitation force had a peak at 0.1 Hz, and the spectrum shape was such that the amplitude decreased smoothly on the lower and higher frequency sides, and the phase was random. The accuracy limit on the high-frequency side of the calculated waveform was assumed to be 2 Hz.

To calculate the simulated tremor waveform by the three-dimensional finite-difference method, the time interval was set to 0.004 s and 132,500 steps (duration of 530 s). The grid interval × number of grids in the difference method was 0.1 km × 840 for each horizontal direction and 0.05 km × 30 + 0.3 km × 80 for the vertical direction. The output of the waveform was set every 20 steps, that is, 0.08 s. In addition, it took about 80 s for the waveform to reach the steady state, so participants were informed that it was desirable to use the waveform after that. The waveform output points were the two sites shown in Fig. 1 (Site A for the shallower base layer and Site C for the deeper base layer) and the inclined base (Site B) connecting them. The data at each site were composed of grid points (33 × 33 points as one data set) in a rectangular area surrounded by 3.2 km × 3.2 km. The coordinates of the centers of Sites A, B, and C (in km) are (32, 42), (42, 42), and (52, 42), respectively. In addition, for the purpose of optional analysis, for the Site B inclination angle of 90°, the rectangular area is extended in the x-direction (direction perpendicular to the inclined plane), and the grid points inside are set to 73 × 33 points.

In the presented procedure, nine sets of simulated microtremor waveforms were created for each of the three cases with different angles of the base slope for the three sites, and they were distributed along with the details of the creation conditions. Participants were asked to submit nine dispersion curves and the analysis conditions for the calculation of the phase velocity in a specified Excel worksheet using each analysis method.

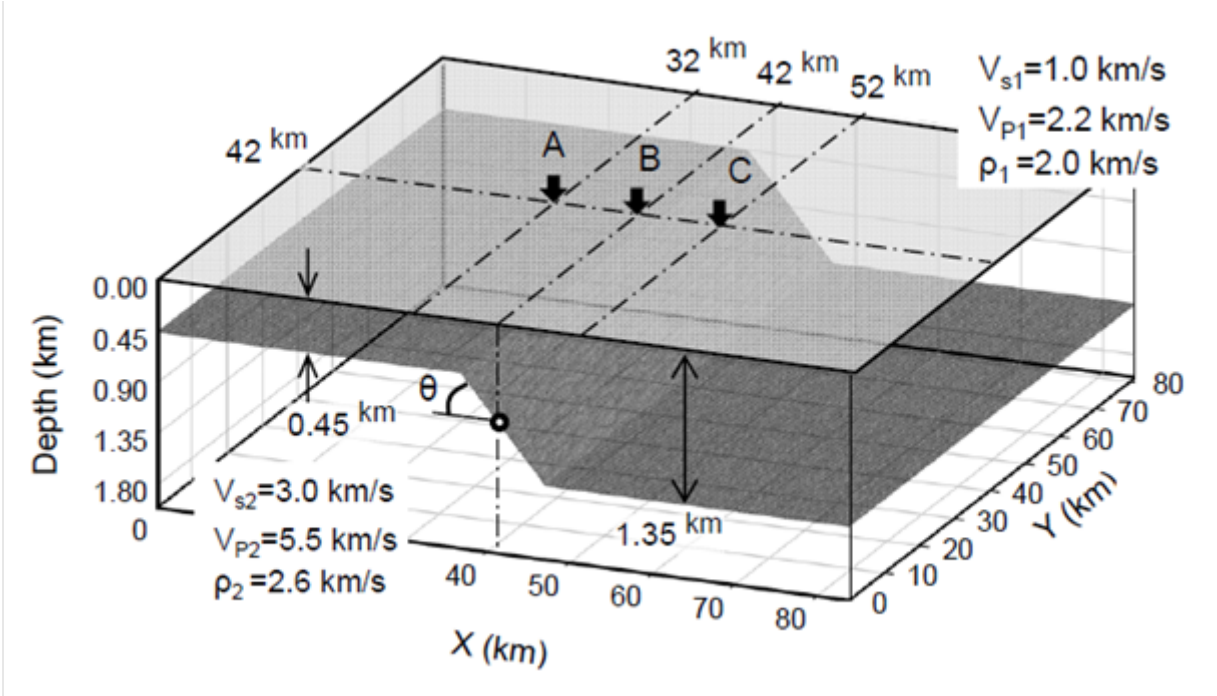

Fig. 1 – Three-dimensional model for simulated microtremor waveform

2.2 Participant submissions

Array analysis methods used by participants include the SPAC method [1], extended SPAC method [33], CCA method [34], and FK method [2, 32]. The methods were expected to be divided into two strains. Therefore, participants were requested that the array layout (Fig. 2) used for analysis be used, Sq5P be used for the SPAC method, and Grid9p be used for the FK method. Eleven participants used the SPAC method, and six used the FK method. In the array analysis, the Rayleigh-wave phase velocity was estimated using the vertical components, and the detailed data of the analysis conditions were submitted along with the calculated phase velocity data. Participants are provided with three component waveforms. As an option, the phase velocities of the Love waves are calculated using the SPAC method [35] or the FK method [36, 37] using the horizontal component. In some cases, different array configurations were used. In this paper, we report the analysis results of the phase velocity using the vertical components that are the requested components (11 sets for the SPAC method and 6 sets for the FK method) and report the analysis results submitted as an option at another opportunity.

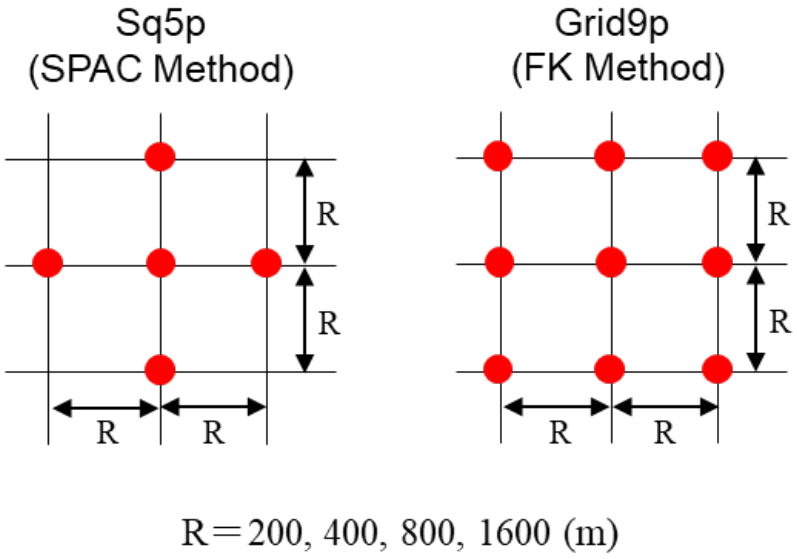

Fig. 2 – Sensor layout for array analyses

2.3 Theoretical value of phase velocity

The theoretical values to be compared with the phase velocities submitted by the participants include the phase velocity of the fundamental mode of the Rayleigh wave [38], the phase velocity considering the higher-order modes of the Rayleigh wave [39], and the phase velocity of the surface wave. In addition, the effective phase velocity [40] of the whole wave field considering both surface waves and body waves is used. When calculating the simulated microtremor waveform by the finite-difference method [26], the physical properties were smoothed near the boundary between the sedimentary layer and the base layer to stabilize the numerical analysis. The thickness of the sedimentary layer immediately below the center was 1.5 grids thinner than the values set in advance for modeling (Site A: 450 m, Site B: 900 m, Site C: 1,350 m). This point was considered when calculating the theoretical value of the phase velocity for the model. Fig. 3 shows the theoretical values of the phase velocity at each site. The phase velocity of the fundamental mode of the Rayleigh wave at each site (referred to as R0 from the Rayleigh wave of the 0th-mode) [38] and the phase velocity considering the higher-order mode of the Rayleigh wave (from the Rayleigh wave of multiple-modes), (called RM) [39] were calculated. The peak appears in the RM near the cutoff frequency of the first mode, and only the fundamental mode exsits in the lower frequency side, so the dispersion curve had an overhang shape. The peak frequency (f_{RM}) of RM was 0.70 Hz for Site A, 0.35 Hz for Site B, and 0.23 Hz for

Site C. Strictly speaking, RM always exceeded R0 on the high-frequency side where higher-order modes appear, but when it was more than about 1.3 times f_{RM}, RM looked almost identical to R0. This frequency named f_{R0} can be observed ataround 0.95 Hz for Site A, 0.48 Hz, and 031 Hz for Site C. In contrast, the phase velocity (called FW from the full-wave field) calculated in consideration of the whole wave field [40] showed a shape that envelops the RM, and its peak frequency appeared on the lower frequency side of f_{RM}, and FW approached R0 as the frequency decreased further. Fig. 3 illustrates f_{FW}, f_{RM}, and f_{R0} for each site.

The peak frequency (f_{FW}) of FW was 0.54 Hz for Site A, 0.26 Hz for Site B, and 0.18 Hz for Site C. The predominant frequency (f_0) for S-wave incidence by one-dimensional wave theory was 0.58 Hz for Site A, 0.28 Hz for Site B, and 0.19 Hz for Site C, and f_{FW} was very close to f_0 within a factor of 1.08. The maximum value of the phase velocity of the FW was almost constant regardless of the site and reached nearly 4 km/s, which is much higher than the S-wave velocity (3 km/s) of the basement layer. The results show that body waves are dominant in the composition of waves near the peak frequency of FW [40].

As described, the simulated microtremor waveform distributed in the benchmark test has a frequency band that includes not only surface waves but also body waves, and the phase velocity calculated from the microtremor array analysis is compared with theoretical ones in Fig. 3. It is of interest which kind of theoretical value corresponds to phase velocity resutls estimated by paticipants.

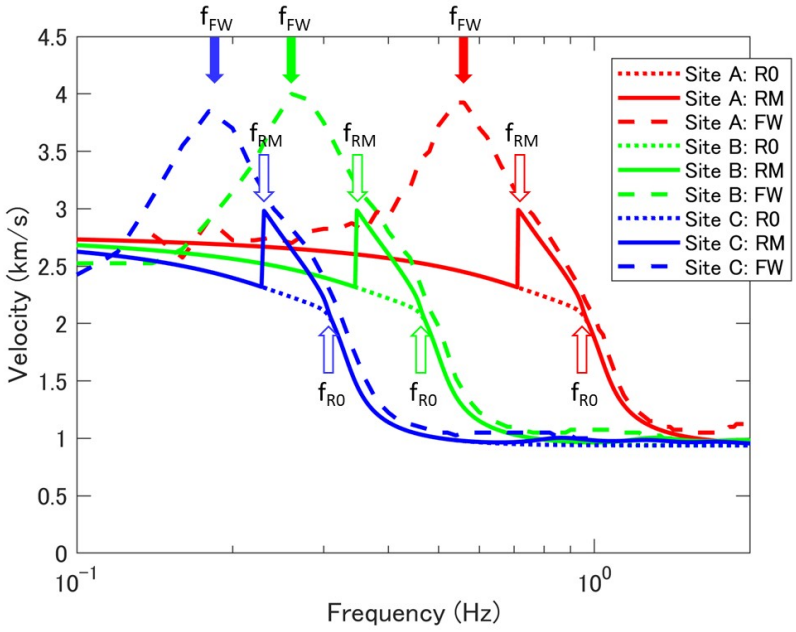

Fig. 3 – Theoretical phase velocities for three sites

3. Phase velocity estimation results and considerations

3.1 Phase velocity by the SPAC method

Fig. 4 shows the phase velocities by the SPAC method. In this figure, the results of each participant are drawn in light blue (labeled RAW). The average value and the average value ± standard deviation are plotted in red (labeled AVR and AVR ± STD). Note that AVR and STD are evaluated when we have more than four teams. Three theoretical values shown in Fig. 3 are also drawn in blue (R0), gray (RM), and ocher (FW). In this figure, nine panels are arranged as 3 × 3. The upper, middle, and lower panes show the results for the inclined angles of 5°, 10°, and 90°, respectively; while the left, center, and right panes show the results for Site A, Site B, and Site C, respectively. Each panel has a label that combines the site and the inclined angle of the subsurface (e.g., Site A/5°). Fig. 5 shows the coefficient of variation (the ratio of standard deviation to

average value) based on the participants' phase velocity results in Fig. 4. In this figure, the results of Site A, Site B, and Site C are aligned from left to right. The features and findings observed from these figures are described in the following paragraphs.

Figs. 4, and 5 show that the phase velocities obtained by the SPAC method tend to have smaller variations as the frequency increases. Regarding the correspondence with the theoretical values, the results are comparable to the theoretical values except for the case where the inclined angle of Site B is 90° (Fig. 4h).

The results of Site A (Fig. 4adg, Fig. 5a) are suitable for observing a relatively wide frequency range from low frequency to high frequency. The figures show that the effect of the inclined angle of the model seems to be trivial and that the estimated phase velocity shows good correspondence to FW.

In Site C, the effect of the inclined angle of the model is not clear (Fig. 4cfi, Fig. 5c), but Site C shows slightly different results from Site A. The results of Site C show that the estimated phase velocities vary greatly at low frequencies below f_{R0} and that the average values seem to correspond better to R0 rather than FW. In Site A, waves mainly come directly from the peripheral source placed on the thin sedimentary layer region. In contrast, in Site C, the wave field seems more complicated, and it consists not only of waves coming directly from the peripheral source placed on the thick sedimentary layer side but also refracted waves or reflected waves because of the existence of the inclined subsurface.

When the inclined angle of Site B is 5° (Fig. 4b), the estimated phase velocity has good correspondence with RM. In addition, when the inclined angle of Site B is 10° (Fig. 4e), the estimated phase velocity has a good correspondence with R0 and shows a low peak at lower frequency than f_{RM}. Note that the characteristics of the estimated phase velocities of Site B differ when the inclined angle increases from 5° to 10°. The results indicate that the phase velocity considering the higher mode of Rayleigh wave [39] becomes noneffective as the inclined angle increases because the inclined angle of the subsurface affects the excitation characteristics of higher-order modes. However, it is presumed that the fundamental mode of the Rayleigh wave is sufficiently excited even at an inclined angle of 10°.

3.2 Phase velocity by the FK method.

Similar to the results for the SPAC method, the results with the FK method are plotted in Figs. 6, 7. Fig. 6 shows the phase velocity obtained using the FK method, and Fig. 7 shows the coefficient of variation. The panel layouts in Fig. 6 are the same as those in Fig. 4. In the following paragraphs, the features and findings observed from these figures are described.

In the case of the FK method, the number of participating teams was smaller than the SPAC method, and the minimum frequency of the phase velocities was around 0.3 Hz. For this reason, the overall characteristics observed in the results of the FK method are similar to those of the SPAC method, but the results of the FK method generally show large variations.

Regarding the correspondence with the theoretical values, similar to the results of the SPAC method, the results of the FK method are comparable to the theoretical values except for the case where the tilt angle of Site B is 90° (Fig. 6h). At Site A, although the variation is large near f_{FW}, the results generally correspond well with the FW (Fig. 6adg and Fig. 7a). The other two results of Site B do not show results around f_{FW}, but they correspond well to FW as a whole (Fig. 6be). In Site C, there is no result near f_{FW}, but the results show good correspondence with FW near f_{RM} on the high-frequency side (Fig. 6cfi and Fig. 7c).

3.3 Other findings

In this benchmark test, even when the inclined angle of Site B was 10°, the variation of the participants' results was small in both the SPAC method and the FK method when the frequency band was slightly higher than f_{RM}, and the correspondence to the theoretical value was good. Thus, the results of the phase velocities obtained from the array analysis can be used in the estimation of the underground structure. In previous studies, the approximation of the stratification structure was considered to be appropriate at an phase velocities obtained from the array analysis can be used in the estimation of the underground structure.

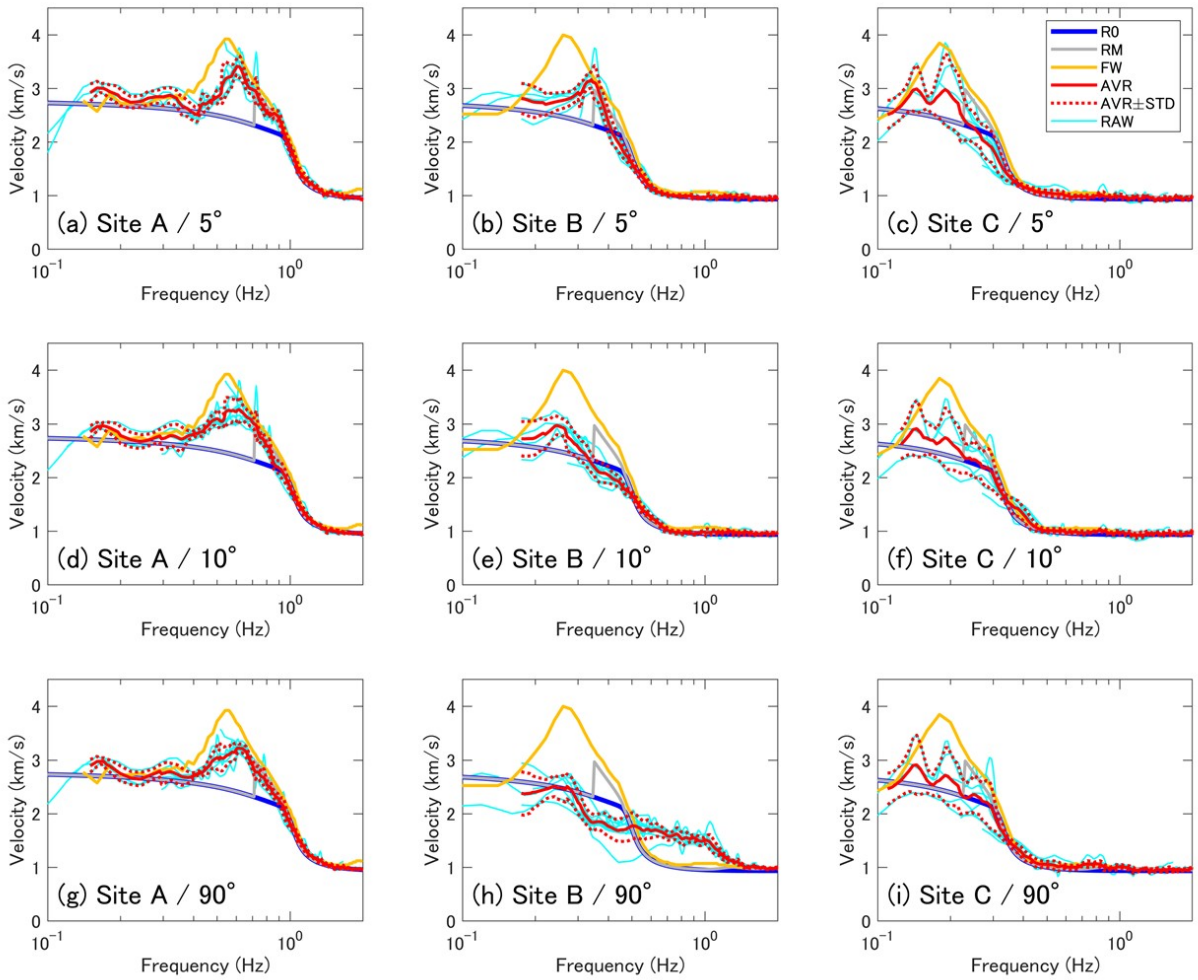

Fig. 4 – Phase velocity results estimated from SPAC method

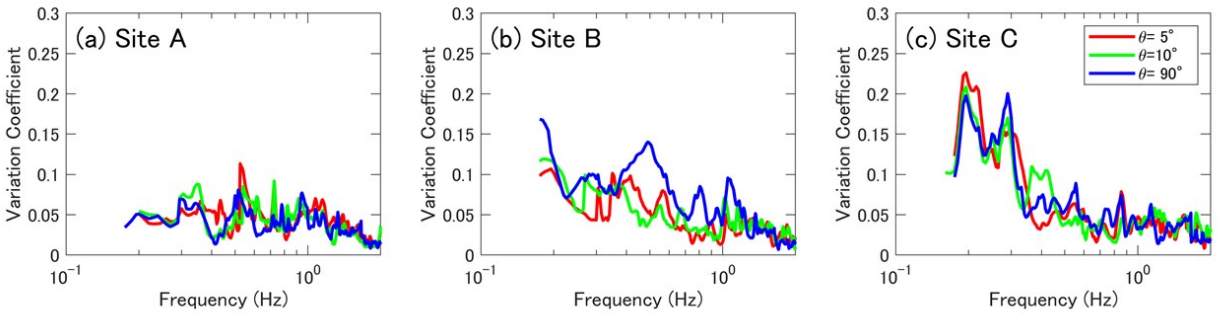

Fig. 5 –Variation coefficients of phase velocity estimated from SPAC method

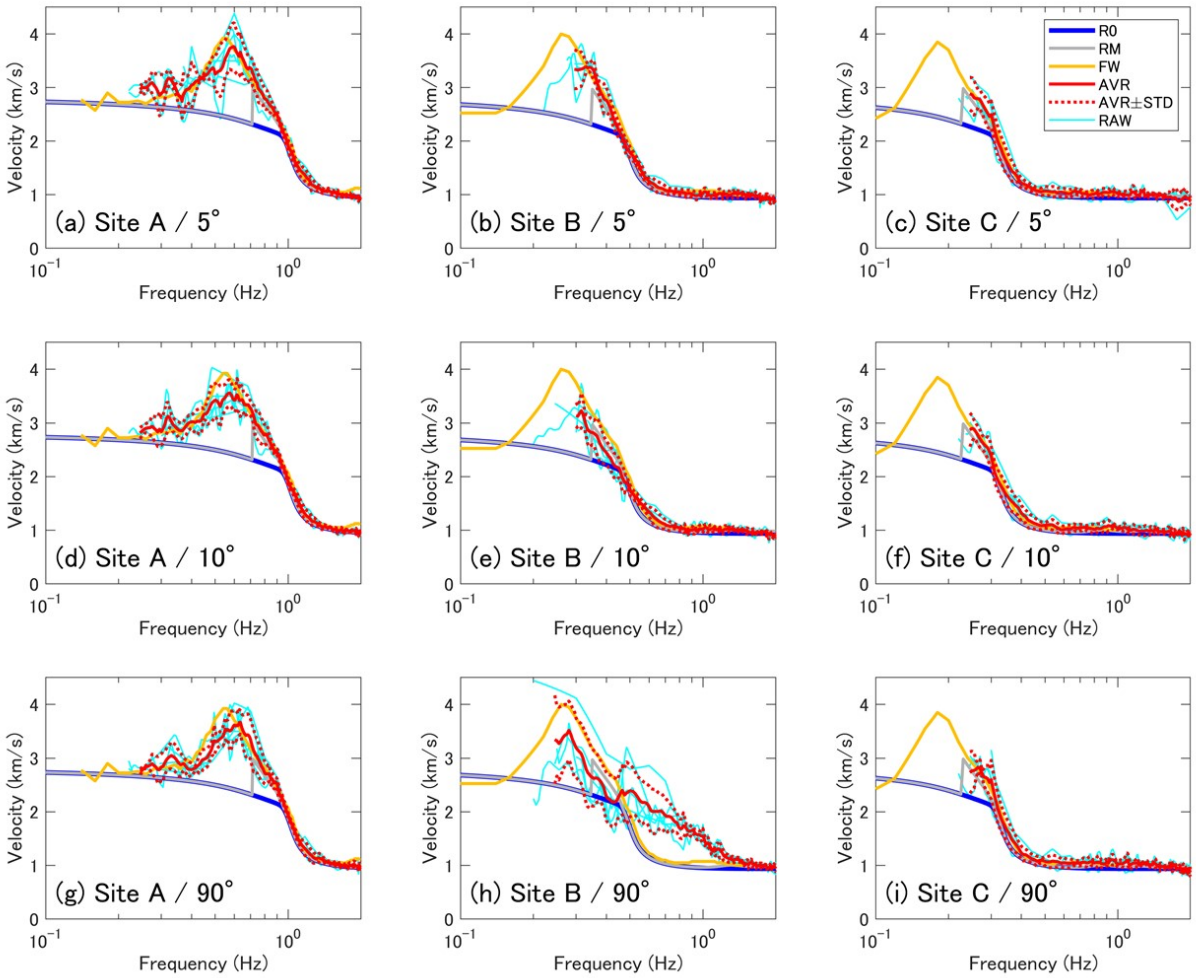

Fig. 6 – Phase velocity results estimated from FK method

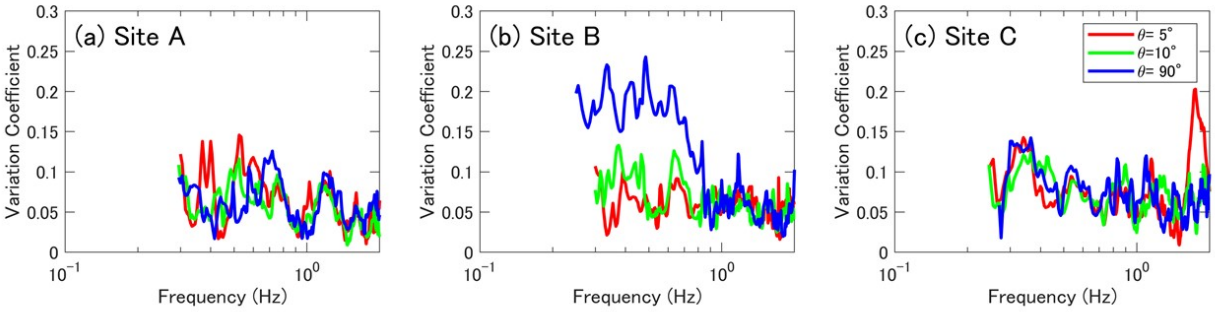

Fig. 7 –Variation coefficients of phase velocity estimated from FK method

phase velocities obtained from the array analysis can be used in the estimation of the underground structure. In previous studies, the approximation of the stratification structure was considered to be appropriate at an inclined angle of about 5° [e.g., 41], but this guideline may be conservative. However, the results of the SPAC method show that the excitability of the higher-order modes varies between the cases of 5° and 10° in inclined angles (Fig. 4be). In contrast, a significant difference is not found in the results of the FK method (Fig. 6be), and the cause should be studied as future work.

In addition, the SPAC and FK methods failed to extract useful phase velocities for estimating underground structures when the inclined angle of Site B was 90°. To remedy this failure, the endpoints of the array arrangement should be offset from the center point of Site B. Through the preceding analysis of the benchmark test and optional analysis by participants, the minimum offset may depend on the array size or the wavelength to be detected. When the subsurface of the bedrock is inclined, single-station observations should be conducted prior to array measurements to grasp the systematic change of the predominant frequency of the horizontal/vertical (H/V) spectrum ratio [10] and to arrange the array carefully.

4. Conclusion

In this study, aiming at clarifying the applicability of the microtremor exploration method on irregular ground, the waveform calculated using the three-dimensional difference-method simulation was regarded as simulated microtremor data, and the participants calculated the phase velocity from the microtremor array analysis. The analysis model was a simple three-dimensional underground structure model in which two horizontal strata were connected by an inclined subsurface structure. As a result, the results show that the estimation result of the phase velocity can be safely used for estimating the underground structure using either the SPAC or FK methods when the inclination angle is about 10°.

In a further study, it is necessary to examine how the estimation parameters can be constrained by considering the phase velocity and the H/V spectrum simultaneously [42]. The phase velocity and the H/V spectrum differ in the change of the error space with respect to the estimated parameters, and it is suggested that the parameter space can be constrained more strongly by considering both [43]. In this project, following the benchmark test introduced in this article, the blind test [21, 22] using the Osaka sedimentary basin model was conducted, in which participants were asked to estimate not only the phase velocity but also the underground structure. Details will be reported in a separate article.

Finally, we describe overall impressions obtained through this project and provide future perspectives. This time, participants who are interested in microtremor array observation and its analysis analyze the same waveform data, compare the analysis conditions and analysis results, and exchange the various know-how in the data processing. For example, the details of analysis conditions, such as how to extract waveforms during spectrum analysis and the types of time windows, also show the perspective of the creator of the analysis code and the tradition inherited in the university laboratory. It seems to give clues to improve the results. In addition, based on a study [20] by the team submitting the results of both the SPAC and FK methods, the analysis results obtained from the FK method get close to those from the SPAC method by selecting the data more than the minimum coherence level (e.g., 0.08 to 0.18). Furthermore, a participant report tells us that horizontal components can be analyzed by a newly proposed FK method other than the previous method [36] [37].

Conrcerned with this project, new research results were generated in the process of analyzing microtremor simulation waveforms. For example, the phase velocity in the full-wave field was newly proposed [40], referred to as FW in this article. While we tested to estimate the phase velocity using the simulated microtremor waveform, we found that the phase velocities showed peak values faster than the S-wave velocities of the bedrock near the S-wave predominant frequency. Making efforts to interpret them led us to a new horizon to investigate the effect of body waves in such a frequency range. When we develop a code for array analysis, we use a simple example waveform such that a plane wave having the phase velocity of the fundamental mode of a Rayleigh wave in a stratified structure propagates from the horizontal direction.

By acquiring an array record by full-scale microtremor simulation in which the microtremor vibration source and underground structure were generated under clear conditions, as in this benchmark test, new results other than the original purpose are expected. Other than the phase velocity in the full-wave field [40], the evaluation of the rotational component from horizontal components and its usage in estimating the Love-wave phase velocity were remarkable wokrs [44]. To share the information with more researchers and technicians, we will publish various data and findings obtained through benchmark tests and blind tests.

Acknowledgments

This work was supported by JSPS KAKENHI Grant Numbers JP19H02287 and JP15H04080. This study was carried out in cooperation with the the working group on evaluation of subsurface structure under the sub committee on ground motion in Architectural Institute of Japan.

Reference

[1] Aki K (1957): Space and time spectra of stationary stochastic waves, with special reference to microtremors, *Bulltein of the Earthquake Research Institute*, **35**, 415-456.

[2] Horike M (1985): Inversion of phase velocity of long-period microtremors to the S-wave-velocity structure down to the basement in urbanized areas, *Journal of Physics in Earth*, **33**, 59-96.

[3] Okada H, Matsushima K, and Hidaka E (1987): Comparison of spatial autocorrelation method and frequency-wavenumber spectral method of estimating the phase velocity of Rayleigh waves in long-period microtremors, *Geophysical Bulltain of Hokkaido University.*, **49**, 53–62 (in Japanese with English abstract).

[4] Okada H (1994): *A research on the practical application of microtremor exploration technique to a wide area survey of a underground structure under 3,000 m in depth*, report of a Grant-in-Aid for Co-operative Research (B) No. 03554009 supported by the Scientific Research Fund in 1993 (in Japanese).

[5] Yamanaka H, Takemura M, Ishida H, Ikeura T, Nozawa T, Sasaki T, and Niwa M (1994): Array measurements of long-period microtremors and estimation of S-wave velocity structure in the western part of the Tokyo metropolitan area, *Zisin 2nd Series*, **47**, 163–172 (in Japanese with English abstract).

[6] Satoh T, Kawase H, and Matsushima S (2001): Estimation of S-wave velocity structures in and around the Sendai Basin, Japan, using array records of microtremors, *Bulltein of the Seismological Society of America*, **91**, 206–218.

[7] Kudo K, Kanno T, Okada H, Ozel O, Erdik M, Sasatani T, Higashi S, Takahashi M, and Yoshida K (2002): Site-specific issues for strong ground motions during the Kocaeli, Turkey, earthquake of 17 August 1999, as inferred from array observations of microtremors and aftershocks, *Bulltein of the Seismological Society of America*, **92**, 448–465.

[8] Kagawa T, Zhao B, Miyakoshi K, and Irikura K (2004): Modeling of 3D Basin Structures for seismic wave simulations based on available information on the target area: case study of the Osaka basin, Japan, *Bulltein of the Seismological Society of America*, **94**, 1353–1368.

[9] Uebayashi H, Ohori M, Kawabe H, Kamae K, Yamada K, Miyakoshi K, Iwata T, Sekigushi H, and Asano K (2018) : Three-dimensional subsurface structure model beneath the Wakayama plain and strong ground motion prediction for the Median Tectonic Line, *Journal of Japan Association for Earthquake Engineering*, **18**, 33-56. (in Japanese with English abstract)

[10] Uebayashi H: Extrapolation of irregular subsurface structures using the horizontal-to-vertical spectral ratio of long-period microtremors, *Bulltein of the Seismological Society of America*, **93**, 570–582, 2003.

[11] Uebayashi H, Kawabe H, Kamae K, Miyakoshi K, and Horike M (2009): Robustness of microtremor H/V spectra in the estimation of an inclined basin-bedrock interface and improvement of the basin model in southern part in Osaka plains, *Journal of Structural and Construction Engineering*, Architectural Institute of Japan, **74**, No. 642, 1453-1460, 33-56. (in Japanese with English abstract)

[12] Motoki K, Watanabe T, Kato K, Takei K, Yamanaka H, Iiba M, and Koyama S (2013): An evaluation of subsurface structure with inclined bedrock using microtrmoer array exploration, *Journal of Structural and Construction Engineering*, AIJ, **78**, No.688, 1081-1088. (in Japanese with English abstract)

[13] Nakagawa H, Hayashida T, Yokoi T, Kashima T, and Koyama S (2015) : A Microtremor exploration in Iwaki city hall for evaluation of inclined bedrock, *Journal of Japan Association for Earthquake Engineering*, **15**, 60-71. (in Japanese with English abstract)

[14] Uebayashi H, Kawabe H, and Kamae K. (2012): Reproduction of microseism H/V spectral features using a three-dimensional complex topographical model of the sediment-bedrock interface in the Osaka sedimentary basin, *Geophysical Journal International*, **189**, 1060-1074.

[15] Arai H, Uebayashi H (2013): Error of bedrock depth estimated from H/V spectrum inversion assuming flat-layered structure at a site in Osaka sedimentary basin, *Summaries of technical papers of Annual Meeting*, Architectural Institute of Japan, B2, 207-208. (in Japanese)

[16] Arai H, Uebayashi H (2014): A study on variation of microseism H/V spectrum due to irregular underground structure in Osaka sedimentary basin, *Summaries of technical papers of Annual Meeting*, Architectural Institute of Japan, B2, 345-346. (in Japanese)

[17] Uebayashi H, Cho I, Ohori M, Nagano M, Arai H (2017): Benchmark test for microtremor array analyses (part1. Equivalent phase velocity in full wavefield), *Summaries of technical papers of Annual Meeting*, Architectural Institute of Japan, B2, 337-338. (in Japanese)

[18] Cho I, Uebayashi H, Ohori M, Nagano M, Arai H, Hagiwara Y, Nobata A, Yokoi T, Hayashida T, Kishi S, Sekiguchi T, Kojima K, Ling S, Nakagawa H, Noguchi T, Suzuki H, Takahashi H, Yoshida K (2017): Benchmark test for microtremor array analyses (part2. Phase velocities by SPAC methods), *Summaries of technical papers of Annual Meeting*, Architectural Institute of Japan, B2, 339-340. (in Japanese)

[19] Ohori M, Uebayashi H, Cho I, Nagano M, Arai H, Hayakawa T, Kishi S, Sekiguchi T, Motoki K, Tsuchida K (2017): Benchmark test for microtremor array analyses (part3. Phase velocities by FK methods), *Summaries of technical papers of Annual Meeting*, Architectural Institute of Japan, B2, 341-342. (in Japanese)

[20] Kishi S, Sekiguchi T, Uebayashi H, Cho I, Ohori M (2017): Study of effect of array shape on estimated phase velocity based on numerical analysis, *Summaries of technical papers of Annual Meeting*, Architectural Institute of Japan, B2, 343-344. (in Japanese)

[21] Uebayashi H, Ohori M, Cho I, Arai H, Yoshida K, Hagiwara Y, Nobata A, Hayashida T, Kishi S, Sekiguchi T, Kojima K, Motoki K, Nakagawa H, Noguchi T, Suzuki H, Takahashi H, Tsuchida K, Nagano M (2018): Benchmark test for microtremor explorations (part1. Velocity structure estimation of the Osaka sedimentary basin), *Summaries of technical papers of Annual Meeting*, Architectural Institute of Japan, B2, 613-614. (in Japanese)

[22] Ohori M, Uebayashi H, Cho I, Arai H, Yoshida K, Hagiwara Y, Nobata A, Hayashida T, Kishi S, Sekiguchi T, Kojima K, Motoki K, Nakagawa H, Noguchi T, Suzuki H, Takahashi H, Tsuchida K, Nagano M (2018): Benchmark test for microtremor explorations (part2. Phase velocity of the Osaka sedimentary basin), *Summaries of technical papers of Annual Meeting*, Architectural Institute of Japan, B2, 615-616. (in Japanese)

[23] Cornou C, Ohmberger M, Boore D M, Kudo K, and Bard P-Y (2006): Derivation of structural models from ambient vibration array recordings: results from an international blind test, *Third Symposium on the Effects of Surface Geology on Seismic Motion*, **2**, 92p., Grenoble, France.

[24] Kudo K (2007): Looking back on local site effect research -ESG research and recent Blind Prediction-, *Proceedings of the 35th Symposium on Ground Vibrations*, Architectural Institute of Japan, 55-64. (in Japanese)

[25] Hisada Y (1995): An efficient method for computing green's functions for a layered half-space with sources and receivers at close depths (Part 2) , *Bulltein of the Seismological Society of America*, **85**, 1080-1093.

[26] Pitarka A (1999): 3D elastic finite-difference modeling of seismic motion using staggered grids with nonuniform spacing, *Bulltein of the Seismological Society of America*, **89**, 54–68.

[27] Foti S, Parolai S, Albarello D, and Picozzi M (2011): Application of surface-wave methods for seismic site characterization, *Surveys in Geophysics*, **32**, 777-825.

[28] Molnar S, Ventura C E, Boroschek R, and Archila M (2015): Site characterization at Chilean strong-motion stations: comparison of downhole and microtremor shear-wave velocity methods, *Soil Dynamics & Earthquake Engineering*, **79**, 22-35.

[29] Garofalo F, Foti S, Hollender F, Bard P-Y, Cornou C, Cox B R, Ohrnberger M, Sicilia D, Asten M, Di Giulio G, Forbriger T, Guillier B, Hayashi K, Martin A, Matsushima S, Mercerat D, Poggi V, and Yamanaka H (2016): InterPACIFIC project: Comparison of invasive and non-invasive methods for seismic site characterization. Part I: Intra-comparison of surface wave methods, *Soil Dynamics & Earthquake Engineering*, **82**, 222–240.

[30] Foti S, Hollender F, Garofalo F, Albarello D, Asten M, Bard P-Y, Comina C, Cornou C, Cox B, Giulio D G, Forbriger T, Hayashi K, Lunedei E, Martin A, Mercerat D, Ohrnberger M, Poggi V, Renalier F, Sicilia D, and Socco V (2018): Guidelines for the good practice of surface wave analysis: A product of the InterPACIFIC project, *Bulltain of Earthquake Engineering*, **16**, 2367–2420.

[31] Asten M W and Hayashi K (2011): Application of the spatial auto-correlation method for shear-wave velocity studies using ambient noise, *Surveys in Geophysics*, **39**, 633–659.

[32] Capon J (1969): High-resolution frequency wavenumber spectrum analysis, *Proc. IEEE*, **57**, 1408-1418.

[33] Ling S, Okada H (1994): Application of the spatial autocorrelation method to a non-circular array for estimation of phase velocities of surface waves in microtremors, *Proceedings of the 91th SEGJ Conference*, 272-275. (in Japanese)

[34] Cho, I., Tada T., and Shinozaki Y.: A Generic formulation for microtremor exploration methods using three-component records from a circular array, *Geophysical Journal International*, **165**, pp. 236-258, 2006.

[35] Matsushima K and Okada H (1990): An exploration method using microtremors (2) -An experiment to identify Love waves in long-period microtremors-, *Proceedings of the 82th SEGJ Conference*, 5-8. (in Japanese with English abstract)

[36] Saito M (2007): Separation of longitudinal and transversal components in microtremors by using a horizontal component seismic array, *BUTSURI-TANSA*, **60**, 297-304. (in Japanese with English abstract)

[37] Tsuchida K, Horike M, Ito S, Hada K (2016): Comparison of the two MLM methods for horizontal component f-k spectra, *Proceedings of the 135th SEGJ Conference*, 97-100. (in Japanese with English abstract)

[38] Harkrider D G (1964): Surface waves in multilayered elastic media I. Rayleigh and Love waves from buried sources in a multilayered elastic half-space, *Bulltein of the Seismological Society of America*, **54**, 627–680.

[39] Tokimatsu K, Tamura S, and Kojima H (1992): Effects of multiple modes on Rayleigh wave dispersion characteristics, *Journal of Geotechnical Engineering*, ASCE, **118**, 1529–1543.

[40] Uebayashi H, Cho I, Ohori M, Yoshida K, Arai H (2020): The effect of body waves on phase-velocity determined by the spatial autocorrelation (SPAC) method, evaluated using full-wave modelling, *Exploration Geophysics*. (https://doi.org/10.1080/08123985.2020.1719825)

[41] Yoshida N (2010): *Earthquake response analysis of ground*, Kajima Institute Publishing Co., LTD., 256p. (in Japanese)

[42] Arai H and Tokimatsu K (2005): S-wave velocity profiling by joint inversion of microtremor dispersion curve and horizontal-to-vertical (H/V) spectrum, *Bulltein of the Seismological Society of America*, **95**, 1766–1778, 2005.

[43] Scherbaum F, Hinzen K-G, and Ohrnberger M (2003): Determination of shallow shear wave velocity profiles in the Cologne, Germany area using ambient vibrations, *Geophysical Journal International*, **152**, 597–612.

[44] Yoshida K and Uebayashi H (2018): Love wave phase velocity estimation by using rotational components obtained from microtremor array records, *BUTSURI-TANSA*, **71**, 15-23. (in Japanese with English abstract)

